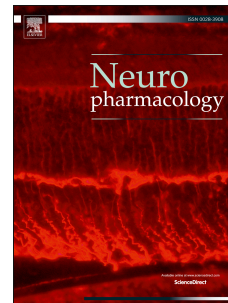


Journal Pre-proof

Mitochondrial malfunction mediates impaired cholinergic Ca²⁺ signalling and submandibular salivary gland dysfunction in diabetes

Olga Kopach, Tetyana Pivneva, Nataliya Fedirko, Nana Voitenko



PII: S0028-3908(23)00379-9

DOI: <https://doi.org/10.1016/j.neuropharm.2023.109789>

Reference: NP 109789

To appear in: *Neuropharmacology*

Received Date: 2 September 2023

Revised Date: 23 October 2023

Accepted Date: 9 November 2023

Please cite this article as: Kopach, O., Pivneva, T., Fedirko, N., Voitenko, N., Mitochondrial malfunction mediates impaired cholinergic Ca²⁺ signalling and submandibular salivary gland dysfunction in diabetes, *Neuropharmacology* (2023), doi: <https://doi.org/10.1016/j.neuropharm.2023.109789>.

This is a PDF file of an article that has undergone enhancements after acceptance, such as the addition of a cover page and metadata, and formatting for readability, but it is not yet the definitive version of record. This version will undergo additional copyediting, typesetting and review before it is published in its final form, but we are providing this version to give early visibility of the article. Please note that, during the production process, errors may be discovered which could affect the content, and all legal disclaimers that apply to the journal pertain.

© 2023 Published by Elsevier Ltd.

Author contributions: Conceptualization: O.K, N.F.; Investigation: O.K., T.P.; Formal analysis: O.K., T.P.; Funding acquisition: N.V.; Methodology: O.K., T.P., N.F., N.V.; Resources: N.V., N.F.; Validation, Visualization: O.K., T.P.; Writing - original draft: O.K.; Review & editing: O.K., T.P, N.V.

Journal Pre-proof

**Mitochondrial malfunction mediates impaired cholinergic Ca²⁺ signalling and
submandibular salivary gland dysfunction in diabetes**

Olga Kopach^{1,2,*}, Tetyana Pivneva^{1,4}, Nataliya Fedirko³, Nana Voitenko^{4,5}

¹ Bogomoletz Institute of Physiology, Kyiv, Ukraine

² Queen Square Institute of Neurology, University College London, London, UK

³ Ivan Franko National University of Lviv, Ukraine

⁴ Kyiv Academic University, Kyiv, Ukraine

⁵ Dobrobut Academy Medical School, Kyiv, Ukraine

Correspondence:

* Dr. Olga Kopach

o.kopach@ucl.ac.uk

UCL Queen Square Institute of Neurology

Queen Square House, London WC1N 3BG

UK

ABSTRACT

Xerostomia (dry-mouth syndrome) is a painful and debilitating condition that frequently occurs in individuals with diabetes and is associated with impaired saliva production and salivary gland hypofunction. Saliva fluid production relies on Ca^{2+} -coupled secretion driven by neurotransmitter stimulation of submandibular acinar cells. Although impairments in intracellular Ca^{2+} signalling have been reported in various xerostomia models, the specific Ca^{2+} -dependent mechanisms underlying saliva fluid hypofunction in diabetes remain unclear. In this study, we show that diabetic animals exhibit severe xerostomia, evident by reduced saliva flow rate, diminished total protein content, and decreased amylase activity in the saliva secreted by submandibular glands. These impairments remained resistant to exogenous cholinergic stimulation. In submandibular acinar cells in diabetes, the intracellular Ca^{2+} signals evoked by cholinergic stimulation were reduced and delayed, caused by malfunctioning mitochondria. Upon initiation of cholinergic-evoked Ca^{2+} signals, mitochondria accumulate higher Ca^{2+} and fail to redistribute Ca^{2+} influx and facilitate the store-operated Ca^{2+} entry effectively. Structural damage to mitochondria was evident in the acinar cells in diabetes. These findings provide insights into the potential targeting of malfunctioning mitochondria for the treatment of diabetic xerostomia as an alternative strategy to the existing pharmacotherapeutic approaches.

**Mitochondrial malfunction mediates impaired cholinergic Ca²⁺ signalling and
submandibular salivary gland dysfunction in diabetes**

Olga Kopach^{1,2,*}, Tetyana Pivneva^{1,4}, Nataliya Fedirko³, Nana Voitenko^{4,5}

¹ Bogomoletz Institute of Physiology, Kyiv, Ukraine

² Queen Square Institute of Neurology, University College London, London, UK

³ Ivan Franko National University of Lviv, Ukraine

⁴ Kyiv Academic University, Kyiv, Ukraine

⁵ Dobrobut Academy Medical School, Kyiv, Ukraine

Correspondence:

* Dr. Olga Kopach

o.kopach@ucl.ac.uk

UCL Queen Square Institute of Neurology

Queen Square House, London WC1N 3BG

UK

ABSTRACT

Xerostomia (dry-mouth syndrome) is a painful and debilitating condition that frequently occurs in individuals with diabetes and is associated with impaired saliva production and salivary gland hypofunction. Saliva fluid production relies on Ca^{2+} -coupled secretion driven by neurotransmitter stimulation of submandibular acinar cells. Although impairments in intracellular Ca^{2+} signalling have been reported in various xerostomia models, the specific Ca^{2+} -dependent mechanisms underlying saliva fluid hypofunction in diabetes remain unclear. In this study, we show that diabetic animals exhibit severe xerostomia, evident by reduced saliva flow rate, diminished total protein content, and decreased amylase activity in the saliva secreted by submandibular glands. These impairments remained resistant to exogenous cholinergic stimulation. In submandibular acinar cells in diabetes, the intracellular Ca^{2+} signals evoked by cholinergic stimulation were reduced and delayed, caused by malfunctioning mitochondria. Upon initiation of cholinergic-evoked Ca^{2+} signals, mitochondria accumulate higher Ca^{2+} and fail to redistribute Ca^{2+} influx and facilitate the store-operated Ca^{2+} entry effectively. Structural damage to mitochondria was evident in the acinar cells in diabetes. These findings provide insights into the potential targeting of malfunctioning mitochondria for the treatment of diabetic xerostomia as an alternative strategy to the existing pharmacotherapeutic approaches.

Keywords: mitochondria, Ca^{2+} signalling, store-operated Ca^{2+} entry, diabetes, acinar cells, saliva secretion.

1. Introduction

Diabetes affects a vast number of individuals globally, surpassing 420 million, and is a severe health condition responsible for approximately 1.5 million deaths annually. Among the various systemic complications that arise from diabetes, xerostomia is as a chronic and debilitating disorder characterised by dry mouth syndrome. This condition is associated with persistent pathological thirst, leading to increased susceptibility to infections, heightened pain sensation, tooth decay, and other related issues (Borgnakke et al., 2015; López-Pintor et al., 2016). Xerostomia and hyposalivation are common early signs of diabetes and prevalent comorbidities found in over half of all diabetes cases (Malicka et al., 2014). However, treating xerostomia remains insufficient primarily due to the unclear mechanisms that mediate salivary gland hypofunction. Xerostomia originates from the inability of acinar cells to synthesise and secrete essential components of saliva (Ambudkar, 2018; Verstappen et al., 2021). Among the three pairs of major salivary glands, the submandibular glands are the primary source of secreted saliva fluid and electrolytes, responsible for maintaining basal saliva secretion to ensure oral moistening (Pedersen et al., 2018).

Human salivary glands produce approximately 1 to 1.5 litres of saliva, predominantly daily through stimulus-driven salivation, a highly regulated process of neurotransmitter-evoked secretion (Melvin et al., 2005). Fluid secretion relies on cholinergic signalling, driven by acetylcholine (ACh) released from the presynaptic terminals of parasympathetic nerves. Activation of muscarinic receptors in the acinar cells facilitates the secretion of fluid and electrolytes (Bymaster et al., 2003; Nakamura et al., 2004; Yamamoto et al., 1996). Therefore, submandibular salivary glands are among the most susceptible organs to the cholinergic (anticholinergic) medication, as they modulate saliva secretion and flow in patients (Arany et al., 2021).

At the cellular level, parasympathomimetics trigger a robust rise in cytosolic Ca^{2+} , which global signal profile is essential for synchronised activation of Ca^{2+} -dependent Cl^- and K^+ channels in polarised acinar cells, ultimately driving saliva fluid secretion (for review, see Lee et al., 2012; Melvin et al., 2005). This intracellular Ca^{2+} rise relies on sustained store-operated Ca^{2+} entry (SOCE) induced by Ca^{2+} release from intracellular Ca^{2+} stores (Parekh and Putney, 2005). Our previous studies (Kopach et al., 2008; Kopach et al., 2011) have demonstrated the vital role of mitochondria in sustaining SOCE and facilitating sufficient Ca^{2+} refilling of the endoplasmic reticulum (ER) through the formation of ' Ca^{2+}

microdomains' – tight contact sites between mitochondria and the ER or plasma membrane. This mitochondrial role is critical for generating Ca^{2+} signals during continuous saliva production following sustained cholinergic stimulation of the submandibular salivary glands, for example, during the tasting and chewing of food when ACh release from parasympathetic nerve terminals increases up to several-fold.

Cumulative evidence indicates that mitochondrial dysfunction represents an early hallmark of various pathologies associated with persistent salivary gland hypofunction. Damaged mitochondrial morphology, including mitochondrial swelling, membrane ruptures, loss and disorganisation of crests, and mitophagosomes, has been reported in patients with the autoimmune disease Sjögren's syndrome (Barrera et al., 2021; Katsiogiannis et al., 2023) and animal models of diabetes mellitus (Huang et al., 2020; Ittichaicharoen et al., 2017; Xiang et al., 2020). Additionally, these pathologies exhibit mitochondrial malfunction, such as membrane depolarisation and increased production of reactive oxygen species (ROS) within the salivary glands. Furthermore, detecting a mitochondrial stress protein in the saliva of type 2 diabetic patients (Yuan et al., 2011) indicates mitochondrial stress as a potential molecular biomarker in saliva secretion.

Mitochondrial malfunction has raised an important question regarding the regulation of intracellular Ca^{2+} signals in the acinar cells of salivary glands in diabetes. Our previous studies have identified that diabetes-induced hyposalivation by the submandibular salivary glands is associated with altered Ca^{2+} release from the ER and suppressed Ca^{2+} -ATPase activity in the plasma membrane and ER in acinar cells (Fedirko et al., 2006). However, the specific connection between malfunctioning mitochondria and compromised SOCE as a potential mechanism for diabetic-induced xerostomia remains unknown. In the present study, we aimed to address this critical question by monitoring cholinergic-induced Ca^{2+} signals in the cytosol and mitochondria using the designed experimental protocols to investigate SOCE upon various stimulation conditions (Kopach et al., 2011) in acinar cells obtained from healthy animals and those with diabetic xerostomia. Our findings indicate that mitochondrial malfunction is the primary cause of the failure of SOCE in diabetes. This failure results in the inability of acinar cells to secrete saliva, subsequently leading to the development of xerostomia.

2. Material and methods

2.1. Animals

Male Wistar rats (150–200 g) were group-housed with water and food available *ad libitum*. The animals were used in accordance with protocols approved by the Animal Care and Use Committee at the Bogomoletz Institute of Physiology. We made every effort to minimise animal suffering and reduce the number of animals used.

2.2. Experimental diabetes

Diabetes was induced by a single administration of streptozotocin (STZ) dissolved in saline (i.p. injection, 60 mg/kg), as described earlier (Fedirko et al., 2006). Saline administration was used as a control. Glucose concentration in blood serum was measured for each animal using a strip-operated blood glucose sensor (Roche Diagnostic, Mannheim, Baden-Württemberg, Germany). The average glucose concentration in blood serum was 6.0 ± 1.0 mM ($n = 20$) for the saline-treated and 22 ± 5 mM ($n = 50$) for the STZ-treated animals. The experiments were conducted 6 weeks after the onset of diabetes.

2.3 Collection of saliva from the submandibular glands; analysis of salivation

The saliva secreted by the submandibular salivary glands was collected using the cannulation method as described in our previous studies (Fedirko et al., 2006; Kopach et al., 2012) and by others (Kuriki et al., 2011). In brief, rats were anaesthetised with i.p. injection of a mixture of ketamine (100 mg/kg, CuraMed Pharma GmbH, Karlsruhe, Germany) and lystenon (0.05 ml/kg, Nycomed GmbH, Austria) and secured in a supine position. To ensure the collection of the saliva secreted by the submandibular glands, cannulation of the Wharton's duct was performed using a glass cannula tightly covering the duct papilla; the cannula was connected with a peristaltic pump to collect the secreted saliva into a small tube (Fig. 1A). To test drug effects on salivation by the submandibular glands, an agonist (or antagonist) was injected into the two glands. Saliva was collected for either 10 min (for an agonist) or 15-20 min (in the case of an antagonist) following the drug administration. For the parasympathetic stimulation of salivation, carbachol was chosen as a parasympathomimetic, as it binds to the same muscarinic receptors as acetylcholine but is resistant to hydrolysis by acetylcholinesterase.

Various parameters were measured, such as saliva flow rate, protein content and amylase activity. The saliva flow rate was defined as the volume of saliva secreted during 1 h normalized to the animal weight. We measured saliva protein content using a classical Lowry

method with spectroscopy and saliva amylase activity via the Caraway method using an amylase-test kit (Biotron Diagnostics, Hemet, CA, USA).

2.4. Preparation of submandibular acinar cells

Deeply anaesthetised animals were decapitated, and the submandibular salivary glands were dissected and placed in a cold HEPES-based extracellular buffer solution. The extracellular buffer solution contained (in mM) NaCl 135, KCl 5, MgCl₂ 2, CaCl₂ 2, HEPES 10, glucose 10 (pH adjusted to 7.35). Acinar cells were enzymatically isolated using collagenase (0.25 mg/ml, 20 to 30 min treatment at 35°C), as described previously (Kopach et al., 2008; Kopach et al., 2011).

2.5. Calcium imaging

2.5.1. Epifluorescence imaging of the cytoplasmic Ca²⁺ level

Isolated acinar cells were bulk loaded with a ratiometric Ca²⁺ dye fura-2/AM by incubating a suspension of freshly isolated cells with the dye (5 μM, 25–30 minutes, 35°C) in the presence of 0.02% pluronic F-127 (Kopach et al., 2008; Kopach et al., 2011; Kopach et al., 2012). After loading the dye, cells were allowed for de-etherification (15-20 min) and then plated on glass coverslips, pre-coated with poly-L-lysine (for 24 h). For imaging, the cells on a coverslip were transferred into a perfusion chamber mounted on an Olympus BX50WI microscope (Olympus Corporation, Japan) fitted with a 60× (0.90 NA) water immersion objective and a highly sensitive 12-bit CCD camera (Sensicam, PCO, Germany). The dye was excited at 340 and 380 nm using a PolyChrome IV monochromator (Till Photonics, Germany) under the control of Imaging Workbench software (INDEC System, USA); emission was recorded at 510 ± 10 nm.

2.5.2. Calibration of cytosolic Ca²⁺ levels

The classical calibration method was performed in the acinar cells using a calcium ionophore ionomycin to determine the intracellular concentration of free Ca²⁺ level ([Ca²⁺]_{cyt}). The experiment involved beginning with zero calcium and gradually increasing the concentration until fura 2 became saturated. Collected images were processed for the background signal subtraction, and [Ca²⁺]_{cyt} values were calculated using the Grynkiewicz equation (Grynkiewicz et al., 1985). All experiments were performed at room temperature (21–23°C).

2.5.3. Ca^{2+} imaging inside the intracellular compartments

For monitoring changes in free Ca^{2+} level within mitochondria ($[Ca^{2+}]_{mit}$), acinar cells were loaded with a low-affinity Ca^{2+} dye rhod-2/AM as we described previously (Kopach et al., 2008; Kopach et al., 2011). A low-affinity Ca^{2+} dye mag-fura-2/AM was used for monitoring the changes in free Ca^{2+} concentration inside the ER ($[Ca^{2+}]_{ER}$) (Kopach et al., 2011; Kopach et al., 2006). For dye loading, a suspension of isolated acinar cells was incubated with rhod-2/AM (5 μ M) or mag-fura-2/AM (6 μ M) for 30-40 minutes at 36-37°C; after dye loading, the cells were allowed to recover (up to 45 min) before starting experiments. To eliminate contamination of fluorescent signal from the intracellular stores by a cytosolic proportion of the dye, we dialysed the cells to wash the cytosolic dye out using a whole-cell configuration as described previously (Kopach et al., 2011). Briefly, cells were patched with a glass pipette filled with (in mM) K-gluconate 133, NaCl 5, $MgCl_2$ 0.5, HEPES/KOH 10, 5 mM EGTA, MgATP 2, NaGTP 0.5 (pH 7.2, osmolarity 280–290 mOsmol). Once in whole-cell, the membrane potential was held at -40 mV using Patch Clamp PC-205B amplifier (Warner Instruments, Hamden, USA) controlled by Clampex 9.2 software (Molecular Devices, USA).

Rhod-2 was excited at 543 nm; emission was recorded at 576 nm. $[Ca^{2+}]_{mit}$ was expressed as the changes in rhod-2 fluorescence at the maximum fluorescent signal over the baseline ($\Delta F/F_0$). The background fluorescence was subtracted for all images. The changes in $[Ca^{2+}]_{ER}$ were expressed as the changes in the ratio of mag-fura-2 fluorescence at 340 nm to those at 380 nm ($\Delta F_{340}/F_{380}$) before and after drug application. For the experiments in Ca^{2+} -free extracellular medium, $CaCl_2$ was omitted, $MgCl_2$ was increased to 4 mM, and 1 mM EGTA was added.

2.6 Electron microscopy

Isolated acinar cells were fixed with 2% paraformaldehyde and 2% glutaraldehyde in 0.1 M phosphate buffer (pH 7.4) for 12 h at 4°C, subsequently rinsed in a cold phosphate buffer and post-fixed in a solution containing 1% of osmium tetroxide. Cells were dehydrated in the increasing series of ethanol, pre-embedded with propylene oxide, and embedded in Epoxide resin (Plano, Wetzlar, Germany). Ultrathin sections were cut (60–70 nm) and processed for post-staining with lead citrate and uranyl acetate. Images were collected with a JEM electron microscope (JEOL, Japan) at 80 kV.

2.7 Data analysis

All datasets were tested for normality using the Shapiro–Wilk test using Origin Pro software. The data distributed normally was presented as mean \pm S.E.M with n referring to the number of cells analysed or animals tested. Statistical significance was calculated using paired and unpaired two-tailed Student's t -test as appropriate or one-way analysis of variance (ANOVA) followed with Bonferroni's post-hoc test. The datasets with normality rejected were presented as median values, and the nonparametric Mann–Whitney test was performed for statistical comparison. A p value of ≤ 0.05 was considered statistically significant for either test.

3. Results

3.1 Hyposalivation and impaired saliva content secreted by the submandibular salivary glands in diabetic xerostomia are resistant to parasympathomimetics

Salivary gland hypofunction is an early indicator of developing diabetes, commonly associated with ongoing thirst, a symptom of xerostomia. To confirm that xerostomia in diabetes is mediated by reduced saliva secretion by the submandibular glands, we analysed various parameters of saliva collected from the gland ducts in both control (healthy) rats and STZ-treated rats. Our analysis showed significant suppression of all tested parameters in STZ-treated rats compared to control animals under basal conditions (no stimulation). Specifically, in diabetes, the saliva flow rate decreased by over 6-fold (median value, 8.4 ml/kg/h, $n = 17$ in control vs 1.2 ml/kg/h, $n = 23$ in STZ-animals, $p = 0.00011^{-3}$, Mann-Whitney test), total saliva protein content decreased by approximately 2-fold (2.5 mg/ml vs 0.3 mg/ml, respectively, $p = 0.000083$, Mann-Whitney test), and total amylase activity decreased by about 3-fold (152 mg/s/l vs 49 mg/s/l, respectively, $p = 0.00091$, Mann-Whitney test; Fig. 1B). These findings indicate a severe reduction in salivation by the submandibular glands, resulting in diabetic xerostomia.

Next, we investigated whether stimulating saliva fluid secretion through activation of muscarinic receptors in salivary cells could alleviate diabetic-induced xerostomia. We administered carbachol (2 μ g/kg), a parasympathomimetic agent resistant to hydrolysis by acetylcholinesterases, and noticed a robust increase in saliva production in all control animals. Carbachol administration significantly increased the saliva flow rate by about 66% (from 9.1 ± 0.9 ml/kg/h to 15.4 ± 1.2 ml/kg/h, $n = 17$, $p = 0.00003$, the two-tailed paired t -test; Fig. 1C-D), protein content – by about 13% (from 2.7 ± 1.4 mg/ml to 3.0 ± 0.2 mg/ml, $n = 17$, $p = 0.0044$, the two-tailed paired t -test; Fig. 1D), and amylase activity – by about 70%

(from 244 ± 59 mg/s/l to 414 ± 79 mg/s/l, $n = 14$, $p < 0.01$, $p = 0.0039$; Fig. 1C-D) compared to basal salivation. However, in all STZ-treated animals, saliva secretion remained dramatically lower even with the stimulation – none of the tested parameters reached the basal level observed in healthy animals. In particular, carbachol administration increased the salivary flow rate in diabetic rats up to 4.7 ± 0.9 ml/kg/h ($n = 13$, $p = 0.0024$, the two-tailed paired t -test; Fig. 1D), protein content to 1.8 ± 0.4 mg/ml ($n = 13$, $p = 0.00049$, the two-tailed paired t -test; Fig. 1D), and amylase activity to 123 ± 10 mg/s/l ($n = 13$; Fig. 1D), but these parameters were still lower than we observed in healthy animals ($p < 0.001$ for the saliva flow rate, $p < 0.05$ for protein content, and $p = 0.064$ for amylase activity, the two-tailed unpaired t -test; Fig. 1D).

Notably, atropine, an anticholinergic agent, suppressed salivation in healthy animals to a level similar to that observed in diabetic rats. Specifically, the salivary flow rate decreased to 2.7 ± 0.3 ml/kg/h ($n = 17$, $p = 0.00087$ ⁻⁸ compared to unstimulated control, the two-tailed paired t -test) and amylase activity dropped to 80 ± 10 mg/s/l ($n = 13$, $p = 0.0002$, the two-tailed paired t -test; Fig. 1C). These results demonstrate the submandibular salivary gland hyposalivation that mediates xerostomia in diabetes and cannot be improved by salivary cell activation with cholinomimetics.

3.2 Impaired cholinergic-evoked $[Ca^{2+}]_{\text{cyt}}$ signals in submandibular acinar cells in diabetes

Saliva fluid secretion relies on increased intracellular Ca^{2+} levels in acinar cells. Because fluid secretion is primarily driven by cholinergic stimulation of salivary cells, we investigated changes in $[Ca^{2+}]_{\text{cyt}}$ signals evoked by the principal neurotransmitter of the parasympathetic nervous system ACh in acinar cells in diabetes. We applied exogenous ACh (5 μ M, 15-30 s) to acinar cells isolated from the submandibular salivary glands of age-matched control and diabetic animals. Our analysis of ACh-induced $[Ca^{2+}]_{\text{cyt}}$ signals revealed significant differences in the amplitude and kinetics of the signals between the two groups (Fig. 2A). The peak amplitude was decreased in diabetes (by $27 \pm 2\%$, $n = 33$ in control and $n = 19$ in diabetes, $p = 0.0027$, the two-tailed unpaired t -test), and the kinetics was slower (the half-rise time prolonged by $113 \pm 13\%$, $p = 0.0006$, and the half-decay time extended by $249 \pm 32\%$, $p = 0.0001$, the two-tailed unpaired t -test; Fig. 2B).

The observed changes were independent of extracellular Ca^{2+} . Even when cells were stimulated with ACh in the absence of extracellular Ca^{2+} , the amplitude remained lower in acinar cells in the diabetic group (248 ± 26 nM, $n = 21$ in control and 187 ± 23 nM, $n = 12$ in

diabetes), and the amplitude decrease was similar between both cohorts (by $22 \pm 2\%$, $n = 21$ and $20 \pm 2\%$, $n = 12$, respectively). The decay kinetics also remained prolonged in Ca^{2+} -free medium in the diabetic group (by $\sim 238\%$, $n = 11$, $p = 0.0025$ compared with control, the two-tailed unpaired t -test). The half-rise time was not significantly different (2.9 ± 0.3 s in control and 3.5 ± 0.5 s in diabetes, $p = 0.371$, the two-tailed unpaired t -test; Fig. 2C). These findings suggest impaired handling of intracellular Ca^{2+} during the signal generation.

Consistent with our previous observations (Fedirko et al., 2006), acinar cells displayed higher levels of resting $[\text{Ca}^{2+}]_{\text{cyt}}$ under diabetic conditions, regardless of whether they were in standard or Ca^{2+} -free medium (Fig. 2A). This further supports impaired cytosolic Ca^{2+} handling in the acinar cells from diabetic animals.

3.3. Higher mitochondrial Ca^{2+} levels in diabetes prevent mitochondria to shape cholinergic-evoked $[\text{Ca}^{2+}]_{\text{cyt}}$ signals

Mitochondrial Ca^{2+} uptake represents a high-capacitive mechanism for rapid Ca^{2+} clearance from the cytoplasm (Duchen et al., 2008). To evaluate how mitochondria contribute to the rearrangement of intracellular Ca^{2+} upon generation of cholinergic-induced $[\text{Ca}^{2+}]_{\text{cyt}}$ signals in acinar cells, we inhibited Ca^{2+} uptake by mitochondria. For the inhibition of mitochondrial Ca^{2+} uniporter, we used a protonophore FCCP ($2 \mu\text{M}$) or a mixture of rotenone ($10 \mu\text{M}$) and oligomycin ($10 \mu\text{M}$), which inhibits mitochondrial respiratory complex I and mitochondrial ATP synthase, depleting cellular ATP level to 64% and 55% of control, respectively (Li et al., 2003). Firstly, we have confirmed that inhibition of mitochondrial Ca^{2+} uptake caused a steady increase of $[\text{Ca}^{2+}]_{\text{cyt}}$ in acinar cells in the control group (Fig. 3A). This increase reflects Ca^{2+} release from mitochondria and is consistent with our previous findings (Kopach et al., 2008; Kopach et al., 2011). However, in the diabetic group, such increase was significantly higher (by $58 \pm 8\%$, $n = 18$, $p = 0.032$ compared with control, Mann-Whitney test). This indicates that mitochondria accumulate higher levels of Ca^{2+} in diabetic conditions. Notably, in the Ca^{2+} -free extracellular medium, $[\text{Ca}^{2+}]_{\text{cyt}}$ rise was lower in acinar cells from the STZ-treated group than in the control (by $58 \pm 8\%$, $n = 3$, $p < 0.01$, the two-tailed unpaired t -test; Fig. 3A), indicating that increased mitochondrial Ca^{2+} accumulation in diabetes is attributed to Ca^{2+} influx.

To assess the role of mitochondria in the generation of cholinergic-evoked $[\text{Ca}^{2+}]_{\text{cyt}}$ signals, we designed the experimental protocol to inhibit mitochondrial Ca^{2+} uptake once the

ACh-induced $[Ca^{2+}]_{cyt}$ signal reached its peak magnitude. This approach enabled us to visualise an amount of Ca^{2+} rapidly accumulated by mitochondria during the signal generation. We observed a robust $[Ca^{2+}]_{cyt}$ elevation, characterised by a slow decay which recovered back to basal level within 5–10 minutes (Fig. 3B). In the STZ-treated group, such $[Ca^{2+}]_{cyt}$ rise had a higher magnitude than in control (by $\sim 57\%$, $n = 4$ in diabetes and $n = 12$ in control, $p < 0.01$, the two-tailed unpaired t -test); its integrated function was also larger (by $\sim 59\%$ compared with control). The rise remained larger in the STZ-treated group when the cells were stimulated in the Ca^{2+} -free extracellular medium (by $\sim 17\%$, $n = 5$ in control and $\sim 30\%$, $n = 3$ in the diabetic group; Fig. 3B).

Having confirmed that mitochondria accumulate higher Ca^{2+} levels upon acinar cell stimulation in diabetes, we next examined how it shapes the Ca^{2+} signal profile. We applied the experimental protocol of stimulating acinar cells with ACh before and after inhibiting mitochondrial Ca^{2+} uptake for paired comparison. The analysis revealed reduced ACh-evoked $[Ca^{2+}]_{cyt}$ signals upon inhibited mitochondrial Ca^{2+} uptake in control cells (by $29 \pm 6\%$, $n = 18$, $p < 0.05$, the two-tailed paired t -test); this reduction was, however, more substantial in diabetes (by $69 \pm 11\%$, $n = 11$, $p < 0.001$, the two-tailed paired t -test; Fig. 3C-D). Also, the signal kinetics was substantially decelerated upon mitochondrial Ca^{2+} uptake inhibition: a decrease in the half-rise time by $\sim 119\%$ ($n = 18$, $p < 0.01$) in control but $\sim 140\%$ ($n = 12$, $p < 0.01$) in the diabetic group. Notably, preventing mitochondrial Ca^{2+} uptake in control cells decelerated the half-rise time to a similar value as in diabetic cells (7.9 ± 1.5 s and 7.7 ± 0.9 s, respectively, Fig. 3D).

3.4. Impaired SOCE and Ca^{2+} refilling of the ER after cholinergic stimulation of acinar cells in diabetes

Ca^{2+} influx is the major source of the intracellular Ca^{2+} rise upon the agonist-induced $[Ca^{2+}]_{cyt}$ signal generation. To investigate whether and how diabetes changes SOCE, we implemented an experimental protocol to visualise SOCE-mediated $[Ca^{2+}]_{cyt}$ rise (Fig. 4A), as in our previous studies (Kopach et al., 2011). In particular, we triggered the ER depletion in a Ca^{2+} -free extracellular medium and subsequently added a Ca^{2+} -containing medium (2 mM) to produce SOCE. Different modes of cell stimulation were tested to mimic either brief or prolonged agonist action, thus, the level of ER depletion. In control cells, the SOCE-mediated $[Ca^{2+}]_{cyt}$ rise depended on the cell stimulation mode, hence more potent stimulation produced larger SOCE ($p < 0.001$, one-way ANOVA with Bonferroni post-hoc test; Fig. 4B). Such a

correlation is entirely consistent with our previous findings (Kopach et al., 2011). Although there was no significant difference in the SOCE amplitude between control and diabetic cells in the case of brief ACh stimulation ($p = 0.184$), more potent stimulation did not result in larger SOCE in diabetes (Fig. 4B). We observed a similar SOCE magnitude in acinar cells between different protocols tested in diabetes ($p = 0.101$, one-way ANOVA with Bonferroni post-hoc test). In particular, the amplitude was ~ 91 nM ($n = 28$) in the case of 30-s ACh, ~ 102 nM ($n = 11$) following SERCA inhibition with thapsigargin (TG, 3 μ M), and ~ 134 nM in the case of 5-min ACh ($n = 22$; Fig. 4B).

In addition to the amplitude, we measured SOCE kinetics, which is thought to more accurately reflect the number of open store-operated Ca^{2+} channels (Glitsch et al., 2002a, b). Again, in contrast to control cells, where the SOCE kinetics depended on the stimulation mode ($p < 0.001$, one-way ANOVA with Bonferroni post-hoc test), in diabetic cells, there was no significant difference in the SOCE kinetics between stimulation protocols (2.3 ± 0.6 s⁻¹, $n = 12$ for 30-s ACh, 2.3 ± 0.5 s⁻¹, $n = 10$ for TG, and 3.6 ± 0.4 s⁻¹, $n = 18$ for 5-min ACh, $p = 0.110$, one-way ANOVA with Bonferroni post-hoc test; Fig. 4B). The similar kinetics suggests a similar number of activated channels in diabetic cells regardless of the stimulation mode.

To validate Ca^{2+} release from the ER following acinar cell stimulation, we visualised the intraluminal Ca^{2+} dynamics in acinar cells of control and diabetic groups using a low-affinity Ca^{2+} dye mag-fura-2/AM. We observed a decrease of $[\text{Ca}^{2+}]_{\text{ER}}$ in response to ACh stimulation (5 μ M, 30 s) in both groups (Fig. 4C). Although ACh stimulation resulted in a drop of $[\text{Ca}^{2+}]_{\text{ER}}$ of a similar magnitude in control and diabetic cells (0.036 ± 0.004 , $n = 11$ and 0.040 ± 0.004 , $n = 6$, respectively, $p = 0.525$, the two-tailed unpaired t -test), the kinetics of $[\text{Ca}^{2+}]_{\text{ER}}$ recovery was dramatically prolonged in diabetes (by $\sim 72\%$ compared with control, $p = 0.010$; Fig. 4D). Sustained ACh stimulation (5 min) produced even more prominent $[\text{Ca}^{2+}]_{\text{ER}}$ response in diabetic cells than in control (0.039 ± 0.005 , $n = 4$ in control vs 0.069 ± 0.007 , $n = 5$ in diabetes, $p = 0.009$, the two-tailed unpaired t -test), and the $[\text{Ca}^{2+}]_{\text{ER}}$ recovery after 5-min stimulation was even more dramatically prolonged in diabetes (by 7-fold compared with that in control, $p = 0.005$, the two-tailed unpaired t -test; Fig. 4D). These data demonstrate severely impaired Ca^{2+} refilling of the ER after cholinergic stimulation of acinar cells in diabetes.

3.5. Malfunctioning mitochondria fail to maintain SOCE

Mitochondrial Ca^{2+} uptake is critical for shaping SOCE and ensuring the adequate Ca^{2+} refiling of the ER upon sustained stimulation of acinar cells (Arnaudeau et al., 2001; Kopach et al., 2011; Liu et al., 2007). We, therefore, further investigated the contribution of malfunctioning mitochondria to impaired SOCE in submandibular acinar cells in diabetes. We applied the same experimental protocol to activate SOCE as described above but inhibited mitochondrial Ca^{2+} uptake after depleting the ER stores (Fig. 5A). Our data revealed that inhibition of mitochondrial Ca^{2+} uptake in the control cells resulted in a similar SOCE magnitude between different protocols tested ($p = 0.120$, one-way ANOVA with Bonferroni post-hoc test). Eventually, mitochondrial inhibition equalised SOCE between control and diabetic cells, so there were no significant differences between the two groups ($p > 0.05$, the two-tailed unpaired t -test) across different stimulation protocols tested (Fig. 5B). Also, the rise slope decelerated to a similar level in control between different SOCE protocols tested ($p = 0.961$, one-way ANOVA with Bonferroni post-hoc test). The kinetics became similar between control and diabetic cells regardless of the protocol tested (30-s ACh: $0.7 \pm 0.2 \text{ s}^{-1}$ and $0.5 \pm 0.1 \text{ s}^{-1}$; TG: $0.8 \pm 0.2 \text{ s}^{-1}$ and $0.8 \pm 0.3 \text{ s}^{-1}$; 5-min ACh: $0.9 \pm 0.2 \text{ s}^{-1}$ and $0.9 \pm 0.3 \text{ s}^{-1}$, respectively). These data indicate that mitochondria determine SOCE in submandibular acinar cells depending on cell stimulation mode and play a key role in SOCE maintenance. The results also confirm that mitochondria are solely responsible for impaired SOCE in diabetes.

To directly visualise the contribution of mitochondrial Ca^{2+} uptake to SOCE maintenance in submandibular acinar cells, we performed monitoring of Ca^{2+} dynamics inside mitochondria during SOCE activation following sustained cholinergic stimulation of the cells (5 min ACh). We visualised $[\text{Ca}^{2+}]_{\text{mit}}$ rise during SOCE activation in control and diabetic cells, which was dramatically lower in diabetic cells (Fig. 5C). The median amplitude of $[\text{Ca}^{2+}]_{\text{mit}}$ rise was 76% ($n = 9$) in the control, but 23% ($n = 11$) in the diabetic group ($p = 0.0031$, Mann-Whitney test; Fig. 5D). The kinetics was also decreased in diabetic conditions (by $\sim 72\%$, $p = 0.001$ compared with control, Mann-Whitney test; Fig. 5D). This further confirms malfunction of mitochondria in acinar cells, resulting in diminished SOCE in diabetes.

3.6. Mitochondrial structural damage in acinar cells in diabetes

To find whether diabetes causes structural changes in acinar cells, especially damage to mitochondria, we next performed EM studies. We observed swelling of submandibular acinar

cells from diabetic rats (Fig. 6A). This was confirmed by counting the basolateral plasma membrane (PM), using 11 separated cuttings obtained from isolated acinar cells of submandibular salivary glands in 3 control and 3 STZ-treated animals. Mean PM was $540 \pm 20 \mu\text{m}$ in 13 cells of the control group but $957 \pm 33 \mu\text{m}$ in 14 cells of the STZ-treated group ($p = 0.0089$, the two-tailed unpaired t -test; Fig. 6B). In the basolateral region, polarised acinar cells contain no secretory granules, which are densely packed in the apical region; therefore, the increased PM in diabetes is due to the cell swelling, regardless of any possible changes in the pool of secretory granules within the apical region.

Given that the initiation of $[\text{Ca}^{2+}]_{\text{cyt}}$ signals, which drive exocytosis in polarised acinar cells, occurs in the basolateral region, we focused on mitochondria and internal mitochondrial structure within the basolateral region. We counted 112 mitochondria in the control ($n = 13$) and 141 mitochondria in the diabetic group ($n = 14$) in the basolateral region of acinar cells. The average area of the mitochondrial membrane, located close to the basal PM, was $56 \pm 1.5 \mu\text{m}^2$ in the control and $77 \pm 3 \mu\text{m}^2$ in the diabetic group ($p = 0.074$, the two-tailed unpaired t -test; Fig. 6B). This indicates mitochondrial swelling in diabetes. Furthermore, individual mitochondria displayed structural damage, including membrane ruptures, numerous vacuolization and considerable damage to mitochondrial cristae, in diabetic conditions (Fig. 6B).

Discussion

Salivary gland dysfunction and hyposalivation are the primary causes of xerostomia, a chronic debilitating condition associated with oral infections, periodontal diseases, tooth loss, and various soft tissue pathologies. Xerostomia (dry mouth syndrome) is one the earliest symptoms of diabetes mellitus, characterised by the acinar cells' inability to produce and secrete saliva. Despite the high prevalence of xerostomia among individuals with diabetes, effective treatments to restore salivary gland function are lacking, and progress in this area is limited due to the unclear mechanisms underlying the development and maintenance of xerostomia at the cellular/subcellular levels. Here, we present evidence highlighting the crucial role of mitochondria in generating intracellular Ca^{2+} signals in acinar cells during cholinergic stimulation of the submandibular salivary glands. Our research shows that mitochondrial Ca^{2+} uptake is essential for sustained SOCE and adequate Ca^{2+} refilling of the

intracellular stores to shape the profile of cholinergic-induced $[Ca^{2+}]_{cyt}$ signals, which are vital for driving Ca^{2+} -dependent secretion.

Among three major salivary glands, the submandibular salivary glands play a key role in saliva fluid secretion, providing continuous saliva outcomes. Using an experimental model of STZ-induced diabetes mellitus, we observed severe xerostomia in STZ-treated rats, characterised by a dramatic decrease of saliva secretion by the submandibular salivary glands. This was evident by severely diminished saliva flow rate (over a 5-fold decrease) and impaired saliva content (decreased total proteins and enzymatic activity), pointing at the primary contribution of submandibular gland dysfunction to diabetes-induced xerostomia. It is important to note that anaesthetics may impact salivation, compromising findings in animal studies where sedation is essential. In clinical practice, ketamine has been known for decades to stimulate oral secretions, hence is often co-administered with anticholinergics to mitigate hypersalivation during sedation (Gingrich, 1994; Heinz et al., 2006). Taking the stimulation effect of ketamine into account, a severity of xerostomia observed in diabetic animals under ketamine-induced sedation, could be even underestimated. Interestingly, hyposalivation persisted despite treatment with carbachol, a cholinomimetic resistant to hydrolysis by acetylcholinesterase, indicating that cholinergic treatment was ineffective in alleviating diabetic-induced xerostomia. This is consistent with our previous findings using other muscarinic receptor agonist pilocarpine (Fedirko et al., 2006). Similar observations have been reported in other xerostomia models, such as Sjögren's syndrome, a systemic autoimmune pathology (Barrera et al., 2021; Katsiougianis et al., 2023; Verstappen et al., 2021) and irradiation-induced salivary gland hypofunction (Liu et al., 2013; Liu et al., 2021).

Saliva secretion is a Ca^{2+} -coupled process, where the generation of neurotransmitter-induced $[Ca^{2+}]_{cyt}$ signals is essential for the sequential activation of spatially localised ion channels and transporters in polarised acinar cells to trigger secretion (Lee et al., 2012; Melvin et al., 2005). Studies have consistently reported impairments in Ca^{2+} signalling in acinar cells of salivary glands in Sjogren's syndrome (Cortés et al., 2019; Dawson et al., 2006; Sun et al., 2023; Teos et al., 2015; Zeng et al., 2017). Similarly, impaired Ca^{2+} signalling in acinar cells of the pancreas is known to cause necrosis, a hallmark of all forms of pancreatitis (Petersen et al., 2021; Voronina and Tepikin, 2012). However, there are not as many reports of salivary cell dysfunction in diabetes (Biswas et al., 2018; Ittichaicharoen et al., 2017). Our previous studies have revealed impaired intracellular Ca^{2+} homeostasis in submandibular acinar cells for the first time in diabetes mellitus (Fedirko et al., 2006). The

present research expands upon our understanding of diabetic-induced impairments in cholinergic-induced $[Ca^{2+}]_{cyt}$ signals by uncovering the mechanism of impaired SOCE and $[Ca^{2+}]_{ER}$ refilling following cholinergic stimulation of acinar cells mediated by malfunctioning mitochondria. Mitochondrial Ca^{2+} uptake is vital to maintain SOCE upon sustained cholinergic stimulation of submandibular acinar cells (Kopach et al., 2011), preventing Ca^{2+} -dependent inactivation of store-operated Ca^{2+} channels (Glitsch et al., 2002b; Rizzuto et al., 2004). In acinar cells, SOCE represents the crucial mechanism of replenishing depleted intracellular Ca^{2+} stores. Following the uptake of Ca^{2+} entering through the store-operated channels, mitochondria subsequently release Ca^{2+} via the mitochondrial Na^+/Ca^{2+} exchanger, enabling Ca^{2+} refilling of the depleted stores – the vital mechanism for acinar cells during sustained stimulation (Kopach et al., 2011). Inhibition of Ca^{2+} entry in salivary gland cells has been proposed as a critical factor contributing to ER stress in Sjogren's syndrome (Sun et al., 2023). Our study has revealed that malfunctioning mitochondria are solely responsible for impaired SOCE in diabetes, resulting in decreased $[Ca^{2+}]_{ER}$ recovery after cholinergic stimulation of acinar cells. Diabetes does not apparently alter the number of store-operated channels but impairs SOCE maintenance due to impaired mitochondria. On the other hand, mitochondrial respiration and ATP production can modulate ion channel conductance.

Previous electron microscopy studies have shown the strategic localization of mitochondria beneath the basolateral PM in acinar cells, allowing mitochondria to rapidly uptake Ca^{2+} entering through store-operated channels, thereby facilitating SOCE (Kopach et al., 2011). Our present data demonstrate that mitochondria accumulate higher Ca^{2+} levels in acinar cells in diabetes, both under resting conditions and upon agonist stimulation. The elevated mitochondrial Ca^{2+} accumulation may be associated with the suppressed activity of Ca^{2+} ATPases in the PM and ER of acinar cells in submandibular salivary glands in diabetes (Fedirko et al., 2006). Mitochondrial Ca^{2+} overload can cause mitochondrial damage, including changes in respiratory capacity and ATP production, thus significantly inhibiting saliva secretion – a process highly dependent on ATP availability. Sustained Ca^{2+} overload can lead to damage in mitochondrial membranes and internal structures. Indeed, our EM microscopy data confirmed damaged mitochondrial structure in acinar cells from diabetic rats, consistent with other reports demonstrating swollen and ruptured mitochondria, vacuolation and dissolution of mitochondria and Golgi elements, and increased lipid

accumulation in intracellular spaces, progressing with the development of diabetes (Huang et al., 2020; Xiang et al., 2020).

Mitochondrial dysfunction is commonly associated with heightened oxidative stress and lipid peroxidation; it also leads to imbalanced production of reactive oxygen species (ROS), reported in salivary glands in STZ-induced diabetes (Biswas et al., 2018; Zalewska et al., 2015), pre-diabetic (obesity) conditions (Ittichaicharoen et al., 2017) and in patients with diabetes mellitus (Al-Rawi, 2011; Su et al., 2012). Mitochondrial membrane depolarisation, accompanied by increased ROS production, leads to impaired intracellular Ca^{2+} signalling in salivary acinar cells, heightened inflammation and apoptosis in obese rats (Ittichaicharoen et al., 2017) and mitophagy in type 2 diabetes (Yamamoto et al., 1996). In addition to impaired Ca^{2+} signals, studies have suggested the link between high levels of ROS and the expression of aquaporins, water channels critical for maintaining water flow and salivary gland fluid secretion (D'Agostino et al., 2020; Soyfoo et al., 2012). Specifically, the suppressed expression of aquaporins 1 and 5 in hyperglycemia (Biswas et al., 2018; Sada et al., 2016) can represent a part of the complex molecular cascades underlying hyposalivation in diabetes. In support of this, experimental aquaporin gene therapy has effectively restored salivary gland function in Sjögren's syndrome (Lai et al., 2016) and irradiation-induced xerostomia (Teos et al., 2016).

Dry mouth syndrome is a common and troublesome condition of diverse etiologies, including radiotherapy, chemotherapies, treatments with neuroactive drugs, various antidepressants, others, and is often associated with medications administered to treat different systemic conditions (Tanasiewicz et al., 2016). Numerous medications with anticholinergic effects can lead to the anticholinergic burden. For instance, muscarinic antagonists, commonly used to treat hyperactivity of visceral smooth muscles, i.e., overactive bladder, cause dry mouth syndrome as a side effect, making it difficult for patients to speak or swallow. Therefore, our experimental findings in diabetic xerostomia may have broader implications for other conditions where similar salivary gland dysfunction occurs via similar impairments of Ca^{2+} signalling. In clinics, targeting muscarinic receptors, i.e. pilocarpine, remains one of only a few options for treating dry mouth syndrome. Despite side effects, this approach is contraindicated in patients taking medications for hypertension, asthma, glaucoma, hyperthyroidism, arrhythmias, some other conditions. Treating xerostomia takes long and new strategies are needed. Our findings provide insights into targeting malfunctioning mitochondria as a potential novel pharmacotherapeutic approach to treating

xerostomia via the mechanism of SOCE-dependent Ca^{2+} -driven saliva fluid secretion. This study describes the mechanism by which impaired mitochondria cause decreased secretion by acinar cells, ultimately resulting in xerostomia. It is important to develop targeted strategies to enhance mitochondrial function, which in turn will protect Ca^{2+} signalling in systemic metabolic syndromes, such as diabetes or other conditions that cause dry mouse syndrome. Previous studies have reported improved salivary gland function in obese rats by targeting oxidative stress and mitochondrial dysfunction (Ittichaicharoen et al., 2018). Similar approaches have also shown promising results by administering mitochondrial scavengers in a model of radiation-induced xerostomia, linking mitochondrial ROS and salivary gland hypofunction (Liu et al., 2021). Altogether, it highlights the potential of addressing mitochondria as a therapeutic target for maintaining persistent salivary gland function in systemic metabolic disorders associated with xerostomia or dry mouth syndrome.

Figure legends

Figure 1. Diabetic-induced xerostomia is resistant to the treatment with cholinomimetics. **(A)** A cartoon showing the cannulation approach for collecting the saliva secreted by the submandibular glands from Wharton's ducts. **(B)** Statistical summary of the saliva parameters in control and diabetic rats: the saliva flow rate, reflecting the secreted saliva volume (left), total saliva protein content (middle), and total amylase activity (right bars). Boxes show median values; $***p < 0.001$, nonparametric Mann-Whitney test. Number of animals tested are indicated. **(C)** Statistical summary of the tested saliva parameters in control rats following cholinergic stimulation with carbachol or anticholinergic treatment with atropine. **(D)** Summary of the saliva parameters in diabetic rats after cholinergic stimulation. Data are mean with s.e.m. $**P < 0.01$; $***p < 0.001$, the two-tailed paired *t*-test; $\#p < 0.05$; $###p < 0.001$, the two-tailed unpaired *t*-test.

Figure 2. Impairments in $[Ca^{2+}]_{cyt}$ signals evoked by cholinergic neurotransmitter stimulation of submandibular acinar cells from diabetic rats.

(A) Representative $[Ca^{2+}]_{cyt}$ signals induced by 5 μ M ACh in Ca^{2+} -containing (left traces) and Ca^{2+} -free (right) extracellular medium in control (black trace) and diabetic (magenta) cells. Image, a snapshot of isolated acinar cells; scale bar, 10 μ m. **(B-C)** Statistical summary of the amplitude (left) and kinetics (middle-right) of ACh-induced $[Ca^{2+}]_{cyt}$ signals in Ca^{2+} -containing **(B)** and Ca^{2+} -free **(C)** extracellular medium. Data are mean with s.e.m. Number of cells tested are indicated. $**P < 0.01$; $***p < 0.001$, the two-tailed unpaired *t*-test.

Figure 3. Mitochondrial Ca^{2+} uptake contributes to $[Ca^{2+}]_{cyt}$ level and shapes cholinergic-induced $[Ca^{2+}]_{cyt}$ signals. **(A)** Representative recordings (left traces) and statistical summary of $[Ca^{2+}]_{cyt}$ rise in acinar cells in the conditions of inhibited mitochondrial Ca^{2+} uptake. Middle panel: bars show median values; $\#p < 0.05$, nonparametric Mann-Whitney test. Right panel: data are mean with s.e.m; $*p < 0.05$, the two-tailed unpaired *t*-test. **(B)** Representative ACh-induced $[Ca^{2+}]_{cyt}$ signals before and after inhibition of mitochondrial Ca^{2+} uptake at the peak of $[Ca^{2+}]_{cyt}$ rise in control (left) and diabetic cells (right). Grey traces are recordings made in Ca^{2+} -free extracellular medium. **(C)** Representative ACh-induced $[Ca^{2+}]_{cyt}$ signals before and following inhibition of mitochondrial Ca^{2+} uptake. Insert shows superimposed ACh-induced $[Ca^{2+}]_{cyt}$ signals in paired recordings (recorded before and following treatment with rotenone and oligomycin (blue line) in control and diabetic cells. **(D)** Statistics of the inhibitory effect on the $[Ca^{2+}]_{cyt}$ signal amplitude (left) and kinetics (right) in control and diabetes. Data are mean with s.e.m. Number of cells tested are indicated. $*P < 0.05$; $**p < 0.01$, the two-tailed paired *t*-test; n.s. non-significant, the two-tailed unpaired *t*-test.

Figure 4. Impaired SOCE in acinar cells from diabetic animals. **(A)**. An experimental protocol of SOCE activation in response to cell stimulation with ACh (5 μ M, 30 s). **(B)** Statistical summary of the amplitudes and kinetics of SOCE-mediated $[Ca^{2+}]_{cyt}$ rise in acinar cells of control and diabetic groups. $*P < 0.05$; $***p < 0.001$, the two-tailed unpaired *t*-test; n.s, non-significant, one-way ANOVA with Bonferroni post-hoc test. **(C)** Representative recordings of $[Ca^{2+}]_{ER}$ responses in mag-fura-2-loaded acinar cells (images on the top panel) to a brief (30-s) ACh application (upper traces) and sustained agonist stimulation (5-min, lower traces) in the control and diabetic groups. **(D)** Statistical summary of the amplitude of $[Ca^{2+}]_{ER}$ response and the kinetics of $[Ca^{2+}]_{ER}$ recovery (ER refiling) following brief (30 s, upper panel) and sustained ACh stimulations (5 min, lower panel) in control and diabetic cells. All data are mean with s.e.m. Number of cells tested are indicated. $**P < 0.01$, n.s, non-significant, the two-tailed unpaired *t*-test.

Figure 5. Malfunctioning mitochondria mediate impaired SOCE in acinar cells in diabetes. **(A)**. Experimental protocol for activating SOCE in the conditions of inhibited mitochondrial Ca^{2+} uptake. Example taken for an acinar cell from SZT-treated rat. **(B)** Statistical summary of SOCE amplitude in the conditions of inhibited mitochondrial Ca^{2+} uptake in the control and diabetic groups for a brief ACh application (left graphs), administration of thapsigargin (TG, middle graphs) and sustained cholinergic stimulation (5-min ACh, right graphs). Data are mean with s.e.m. Number of cells tested are indicated. **(C)**. Top panel shows images of acinar cells loaded with Rhod-2 for monitoring changes in $[Ca^{2+}]_{mit}$ during SOCE activation. Dotted line highlights a patched acinar cell before and following SOCE activation. Traces show representative $[Ca^{2+}]_{mit}$ recordings during SOCE activation by sustained stimulation (ACh, 5 min) of acinar cells in control and diabetes. **(D)**. Statistical summary of the $[Ca^{2+}]_{mit}$ amplitude and kinetics in acinar cells from control and diabetic animals. Boxes show median values; $**p < 0.01$, $***p < 0.001$, nonparametric Mann-Whitney test.

Figure 6. Diabetes causes structural changes in acinar cells of submandibular salivary glands. **(A)** Representative EM images showing subcellular structure of acinar cells from submandibular salivary glands in control (left) and STZ-treated rats (right). Insert on A shows an enlarged view of mitochondria (mit) located close to the basolateral plasma membrane (PM) and surrounded by the ER. Nuc, nuclei. Scale bars, 1 μ m. **(B)** Left bars, statistical summary of the basolateral PM length (upper) and mitochondrial area (lower) in control and diabetes. Right images show mitochondrial damage and swelling crests (arrows) in acinar cells from diabetic rats. Scale bars 0.5 μ m; for inserts, 100 nm. Data are mean with s.e.m. Number of cells are indicated. $**P < 0.01$, the two-tailed unpaired *t*-test.

References

- Al-Rawi, N. H., 2011. Oxidative stress, antioxidant status and lipid profile in the saliva of type 2 diabetics. *Diab Vasc Dis Res* 8, 22-28.
- Ambudkar, I., 2018. Calcium signaling defects underlying salivary gland dysfunction. *Biochim Biophys Acta Mol Cell Res* 1865, 1771-1777.
- Arany, S., Kopycka-Kedzierawski, D. T., Caprio, T. V., Watson, G. E., 2021. Anticholinergic medication: Related dry mouth and effects on the salivary glands. *Oral Surg Oral Med Oral Pathol Oral Radiol* 132, 662-670.
- Arnaudeau, S., Kelley, W. L., Walsh, J. V., Jr., Demaurex, N., 2001. Mitochondria recycle Ca^{2+} to the endoplasmic reticulum and prevent the depletion of neighboring endoplasmic reticulum regions. *J Biol Chem* 276, 29430-29439.
- Barrera, M. J., Aguilera, S., Castro, I., Carvajal, P., Jara, D., Molina, C., González, S., González, M. J., 2021. Dysfunctional mitochondria as critical players in the inflammation of autoimmune diseases: Potential role in Sjögren's syndrome. *Autoimmun Rev* 20, 102867.
- Biswas, R., Ahn, J. C., Moon, J. H., Kim, J., Choi, Y. H., Park, S. Y., Chung, P. S., 2018. Low-level laser therapy with 850 nm recovers salivary function via membrane redistribution of aquaporin 5 by reducing intracellular Ca^{2+} overload and ER stress during hyperglycemia. *Biochim Biophys Acta Gen Subj* 1862, 1770-1780.
- Borgnakke, W. S., Anderson, P. F., Shannon, C., Jivanescu, A., 2015. Is there a relationship between oral health and diabetic neuropathy? *Curr Diab Rep* 15, 93.
- Bymaster, F. P., Carter, P. A., Yamada, M., Gomeza, J., Wess, J., Hamilton, S. E., Nathanson, N. M., McKinzie, D. L., Felder, C. C., 2003. Role of specific muscarinic receptor subtypes in cholinergic parasympathomimetic responses, in vivo phosphoinositide hydrolysis, and pilocarpine-induced seizure activity. *Eur J Neurosci* 17, 1403-1410.
- Cortés, J., Hidalgo, J., Aguilera, S., Castro, I., Brito, M., Urrea, H., Pérez, P., Barrera, M. J., Carvajal, P., Urzúa, U., González, S., Molina, C., Bahamondes, V., Hermoso, M., González, M. J., 2019. Synaptotagmin-1 overexpression under inflammatory conditions affects secretion in salivary glands from Sjögren's syndrome patients. *J Autoimmun* 97, 88-99.
- D'Agostino, C., Elkashty, O. A., Chivasso, C., Perret, J., Tran, S. D., Delporte, C., 2020. Insight into Salivary Gland Aquaporins. *Cells* 9.
- Dawson, L. J., Stanbury, J., Venn, N., Hasdimir, B., Rogers, S. N., Smith, P. M., 2006. Antimuscarinic antibodies in primary Sjögren's syndrome reversibly inhibit the mechanism of fluid secretion by human submandibular salivary acinar cells. *Arthritis Rheum* 54, 1165-1173.
- Duchen, M. R., Verkhatsky, A., Muallem, S., 2008. Mitochondria and calcium in health and disease. *Cell Calcium* 44, 1-5.
- Fedirko, N. V., Kruglikov, I. A., Kopach, O. V., Vats, J. A., Kostyuk, P. G., Voitenko, N. V., 2006. Changes in functioning of rat submandibular salivary gland under streptozotocin-induced diabetes are associated with alterations of Ca^{2+} signaling and Ca^{2+} transporting pumps. *Biochim Biophys Acta* 1762, 294-303.
- Glitsch, M. D., Bakowski, D., Parekh, A. B., 2002a. Effects of inhibitors of the lipo-oxygenase family of enzymes on the store-operated calcium current $I(\text{CRAC})$ in rat basophilic leukaemia cells. *J Physiol* 539, 93-106.
- Gingrich, B.K., 1994. Difficulties encountered in a comparative study of orally administered midazolam and ketamine [letter]. *Anesthesiology* 80, 1414.
- Glitsch, M. D., Bakowski, D., Parekh, A. B., 2002b. Store-operated Ca^{2+} entry depends on mitochondrial Ca^{2+} uptake. *Embo j* 21, 6744-6754.

- Gryniewicz, G., Poenie, M., Tsien, R. Y., 1985. A new generation of Ca²⁺ indicators with greatly improved fluorescence properties. *J Biol Chem* 260, 3440-3450.
- Heinz, P., Geelhoed, G.C., Wee, C., Pascoe, E.M., 2006. Is atropine needed with ketamine sedation? A prospective, randomized, double blind study. *Emerg Med J.* 23, 206–9.
- Huang, Y., Mao, Q. Y., Shi, X. J., Cong, X., Zhang, Y., Wu, L. L., Yu, G. Y., Xiang, R. L., 2020. Disruption of tight junctions contributes to hyposalivation of salivary glands in a mouse model of type 2 diabetes. *J Anat* 237, 556-567.
- Ittichaicharoen, J., Apaijai, N., Tanajak, P., Sa-Nguanmoo, P., Chattipakorn, N., Chattipakorn, S., 2018. Dipeptidyl peptidase-4 inhibitor enhances restoration of salivary glands impaired by obese-insulin resistance. *Arch Oral Biol* 85, 148-153.
- Ittichaicharoen, J., Apaijai, N., Tanajak, P., Sa-Nguanmoo, P., Chattipakorn, N., Chattipakorn, S. C., 2017. Impaired mitochondria and intracellular calcium transients in the salivary glands of obese rats. *Appl Physiol Nutr Metab* 42, 420-429.
- Katsiogiannis, S., Stergiopoulos, A., Moustaka, K., Havaki, S., Samiotaki, M., Stamatakis, G., Tenta, R., Skopouli, F. N., 2023. Salivary gland epithelial cell in Sjögren's syndrome: Metabolic shift and altered mitochondrial morphology toward an innate immune cell function. *J Autoimmun* 136, 103014.
- Kopach, O., Kruglikov, I., Pivneva, T., Voitenko, N., Fedirko, N., 2008. Functional coupling between ryanodine receptors, mitochondria and Ca(2+) ATPases in rat submandibular acinar cells. *Cell Calcium* 43, 469-481.
- Kopach, O., Kruglikov, I., Pivneva, T., Voitenko, N., Verkhatsky, A., Fedirko, N., 2011. Mitochondria adjust Ca(2+) signaling regime to a pattern of stimulation in salivary acinar cells. *Biochim Biophys Acta* 1813, 1740-1748.
- Kopach, O., Vats, J., Netsyk, O., Voitenko, N., Irving, A., Fedirko, N., 2012. Cannabinoid receptors in submandibular acinar cells: functional coupling between saliva fluid and electrolytes secretion and Ca²⁺ signalling. *J Cell Sci* 125, 1884-1895.
- Kopach, O. V., Kruhlykov, I. A., Kostiuk, P. H., Voitenko, N. V., Fedirko, N. V., 2006. Characteristics of inositoltrisphosphate-sensitive Ca²⁺ stores in the acinar cells of rat submandibular salivary gland. *Fiziol Zh* 52, 30-40.
- Kuriki, Y., Liu, Y., Xia, D., Gjerde, E. M., Khalili, S., Mui, B., Zheng, C., Tran, S. D., 2011. Cannulation of the mouse submandibular salivary gland via the Wharton's duct. *J Vis Exp*.
- Lai, Z., Yin, H., Cabrera-Pérez, J., Guimaro, M. C., Afione, S., Michael, D. G., Glenton, P., Patel, A., Swaim, W. D., Zheng, C., Nguyen, C. Q., Nyberg, F., Chiorini, J. A., 2016. Aquaporin gene therapy corrects Sjögren's syndrome phenotype in mice. *Proc Natl Acad Sci U S A* 113, 5694-5699.
- Lee, M. G., Ohana, E., Park, H. W., Yang, D., Muallem, S., 2012. Molecular mechanism of pancreatic and salivary gland fluid and HCO₃ secretion. *Physiol Rev* 92, 39-74.
- Li, N., Ragheb, K., Lawler, G., Sturgis, J., Rajwa, B., Melendez, J.A., Robinson, J.P., 2003. Mitochondrial complex I inhibitor rotenone induces apoptosis through enhancing mitochondrial reactive oxygen species production. *J Biol Chem* 278 (10), 8516-8525.
- Liu, X., Cheng, K. T., Bandyopadhyay, B. C., Pani, B., Dietrich, A., Paria, B. C., Swaim, W. D., Beech, D., Yildirim, E., Singh, B. B., Birnbaumer, L., Ambudkar, I. S., 2007. Attenuation of store-operated Ca²⁺ current impairs salivary gland fluid secretion in TRPC1(-/-) mice. *Proc Natl Acad Sci U S A* 104, 17542-17547.
- Liu, X., Cotrim, A., Teos, L., Zheng, C., Swaim, W., Mitchell, J., Mori, Y., Ambudkar, I., 2013. Loss of TRPM2 function protects against irradiation-induced salivary gland dysfunction. *Nat Commun* 4, 1515.
- Liu, X., Subedi, K. P., Zheng, C., Ambudkar, I., 2021. Mitochondria-targeted antioxidant protects against irradiation-induced salivary gland hypofunction. *Sci Rep* 11, 7690.

- López-Pintor, R. M., Casañas, E., González-Serrano, J., Serrano, J., Ramírez, L., de Arriba, L., Hernández, G., 2016. Xerostomia, Hyposalivation, and Salivary Flow in Diabetes Patients. *J Diabetes Res* 2016, 4372852.
- Malicka, B., Kaczmarek, U., Skośkiewicz-Malinowska, K., 2014. Prevalence of xerostomia and the salivary flow rate in diabetic patients. *Adv Clin Exp Med* 23, 225-233.
- Melvin, J. E., Yule, D., Shuttleworth, T., Begenisich, T., 2005. Regulation of fluid and electrolyte secretion in salivary gland acinar cells. *Annu Rev Physiol* 67, 445-469.
- Nakamura, T., Matsui, M., Uchida, K., Futatsugi, A., Kusakawa, S., Matsumoto, N., Nakamura, K., Manabe, T., Taketo, M. M., Mikoshiba, K., 2004. M(3) muscarinic acetylcholine receptor plays a critical role in parasympathetic control of salivation in mice. *J Physiol* 558, 561-575.
- Parekh, A. B., Putney, J. W., Jr., 2005. Store-operated calcium channels. *Physiol Rev* 85, 757-810.
- Pedersen, A. M. L., Sørensen, C. E., Proctor, G. B., Carpenter, G. H., Ekström, J., 2018. Salivary secretion in health and disease. *J Oral Rehabil* 45, 730-746.
- Petersen, O. H., Gerasimenko, J. V., Gerasimenko, O. V., Gryshchenko, O., Peng, S., 2021. The roles of calcium and ATP in the physiology and pathology of the exocrine pancreas. *Physiol Rev* 101, 1691-1744.
- Rizzuto, R., Duchen, M. R., Pozzan, T., 2004. Flirting in little space: the ER/mitochondria Ca²⁺ liaison. *Sci STKE* 2004, re1.
- Sada, K., Nishikawa, T., Kukidome, D., Yoshinaga, T., Kajihara, N., Sonoda, K., Senokuchi, T., Motoshima, H., Matsumura, T., Araki, E., 2016. Hyperglycemia Induces Cellular Hypoxia through Production of Mitochondrial ROS Followed by Suppression of Aquaporin-1. *PLoS One* 11, e0158619.
- Soyfoo, M. S., Bolaky, N., Depoortere, I., Delporte, C., 2012. Relationship between aquaporin-5 expression and saliva flow in streptozotocin-induced diabetic mice? *Oral Dis* 18, 501-505.
- Su, H., Velly, A. M., Salah, M. H., Benarroch, M., Trifiro, M., Schipper, H. M., Gornitsky, M., 2012. Altered redox homeostasis in human diabetes saliva. *J Oral Pathol Med* 41, 235-241.
- Tanasiewicz, M., Hildebrandt, T., Obersztyn, I., 2016. Xerostomia of Various Etiologies: A Review of the Literature. *Adv Clin Exp Med* 25(1), 199-206.
- Sun, Y., Nascimento Da Conceicao, V., Chauhan, A., Sukumaran, P., Chauhan, P., Ambrus, J. L., Vissink, A., Kroese, F. G. M., Muniswamy, M., Mishra, B. B., Singh, B. B., 2023. Targeting alarmin release reverses Sjogren's syndrome phenotype by revitalizing Ca(2+) signalling. *Clin Transl Med* 13, e1228.
- Teos, L. Y., Zhang, Y., Cotrim, A. P., Swaim, W., Won, J. H., Ambrus, J., Shen, L., Bebris, L., Grisius, M., Jang, S. I., Yule, D. I., Ambudkar, I. S., Alevizos, I., 2015. IP3R deficit underlies loss of salivary fluid secretion in Sjögren's Syndrome. *Sci Rep* 5, 13953.
- Teos, L. Y., Zheng, C. Y., Liu, X., Swaim, W. D., Goldsmith, C. M., Cotrim, A. P., Baum, B. J., Ambudkar, I. S., 2016. Adenovirus-mediated hAQP1 expression in irradiated mouse salivary glands causes recovery of saliva secretion by enhancing acinar cell volume decrease. *Gene Ther* 23, 572-579.
- Verstappen, G. M., Pringle, S., Bootsma, H., Kroese, F. G. M., 2021. Epithelial-immune cell interplay in primary Sjögren syndrome salivary gland pathogenesis. *Nat Rev Rheumatol* 17, 333-348.
- Voronina, S., Tepikin, A., 2012. Mitochondrial calcium in the life and death of exocrine secretory cells. *Cell Calcium* 52, 86-92.
- Xiang, R. L., Huang, Y., Zhang, Y., Cong, X., Zhang, Z. J., Wu, L. L., Yu, G. Y., 2020. Type 2 diabetes-induced hyposalivation of the submandibular gland through PINK1/Parkin-mediated mitophagy. *J Cell Physiol* 235, 232-244.

Yamamoto, H., Sims, N. E., Macauley, S. P., Nguyen, K. H., Nakagawa, Y., Humphreys-Beher, M. G., 1996. Alterations in the secretory response of non-obese diabetic (NOD) mice to muscarinic receptor stimulation. *Clin Immunol Immunopathol* 78, 245-255.

Yuan, J., Dunn, P., Martinus, R. D., 2011. Detection of Hsp60 in saliva and serum from type 2 diabetic and non-diabetic control subjects. *Cell Stress Chaperones* 16, 689-693.

Zalewska, A., Knaś, M., Maciejczyk, M., Waszkiewicz, N., Klimiuk, A., Choromańska, M., Matczuk, J., Waszkiel, D., Car, H., 2015. Antioxidant profile, carbonyl and lipid oxidation markers in the parotid and submandibular glands of rats in different periods of streptozotocin induced diabetes. *Arch Oral Biol* 60, 1375-1386.

Zeng, M., Szymczak, M., Ahuja, M., Zheng, C., Yin, H., Swaim, W., Chiorini, J. A., Bridges, R. J., Muallem, S., 2017. Restoration of CFTR Activity in Ducts Rescues Acinar Cell Function and Reduces Inflammation in Pancreatic and Salivary Glands of Mice. *Gastroenterology* 153, 1148-1159.

Data Statement: All data generated and/or analysed during this study are included in this article.

Declaration of interest: none.

Author contributions: Conceptualization: O.K., N.F.; Investigation: O.K., T.P.; Formal analysis: O.K., T.P.; Funding acquisition: N.V.; Methodology: O.K., T.P., N.F., N.V.; Resources: N.V., N.F.; Validation, Visualization: O.K., T.P.; Writing - original draft: O.K.; Review & editing: O.K., T.P, N.V.

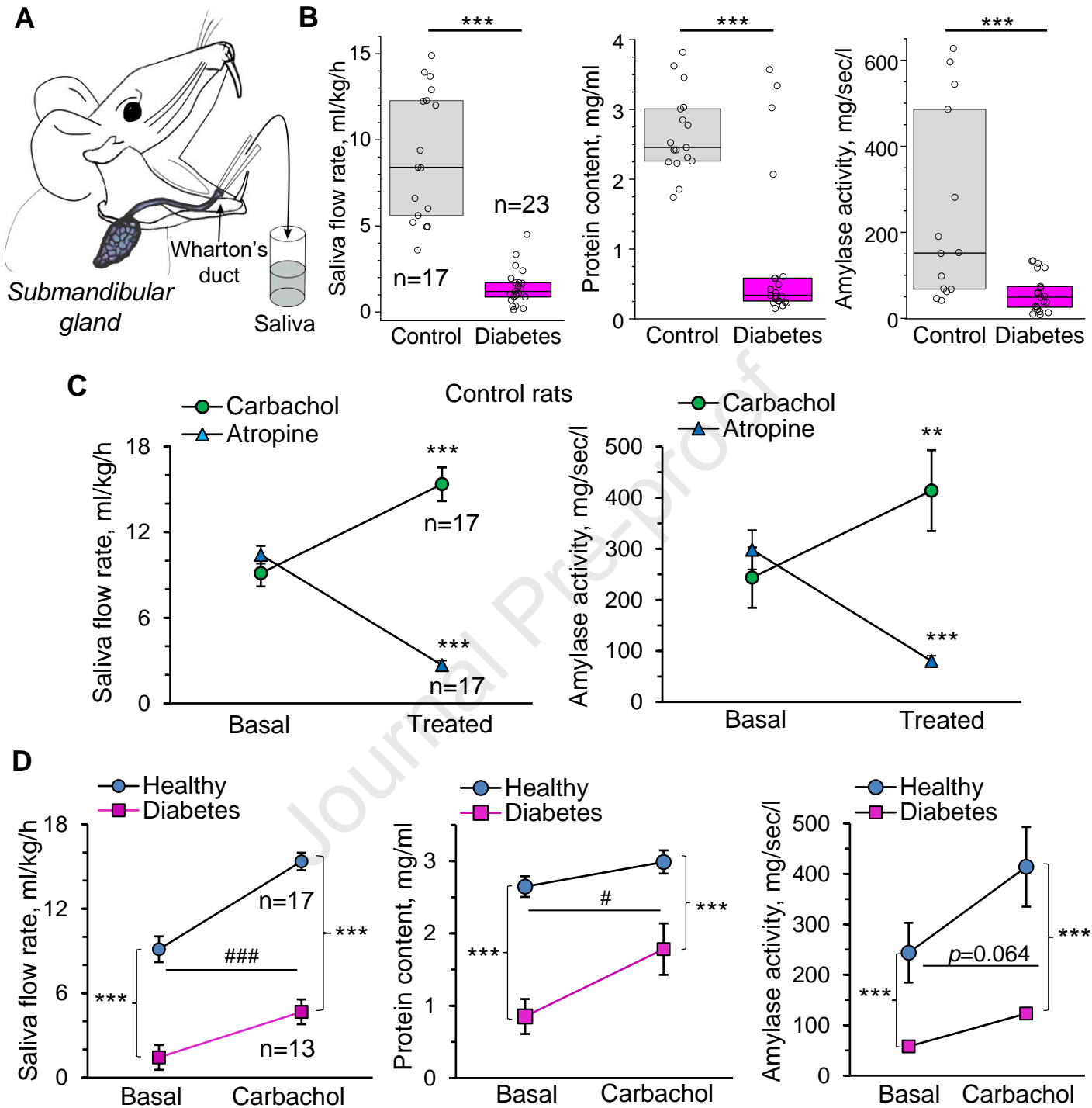


Figure 1

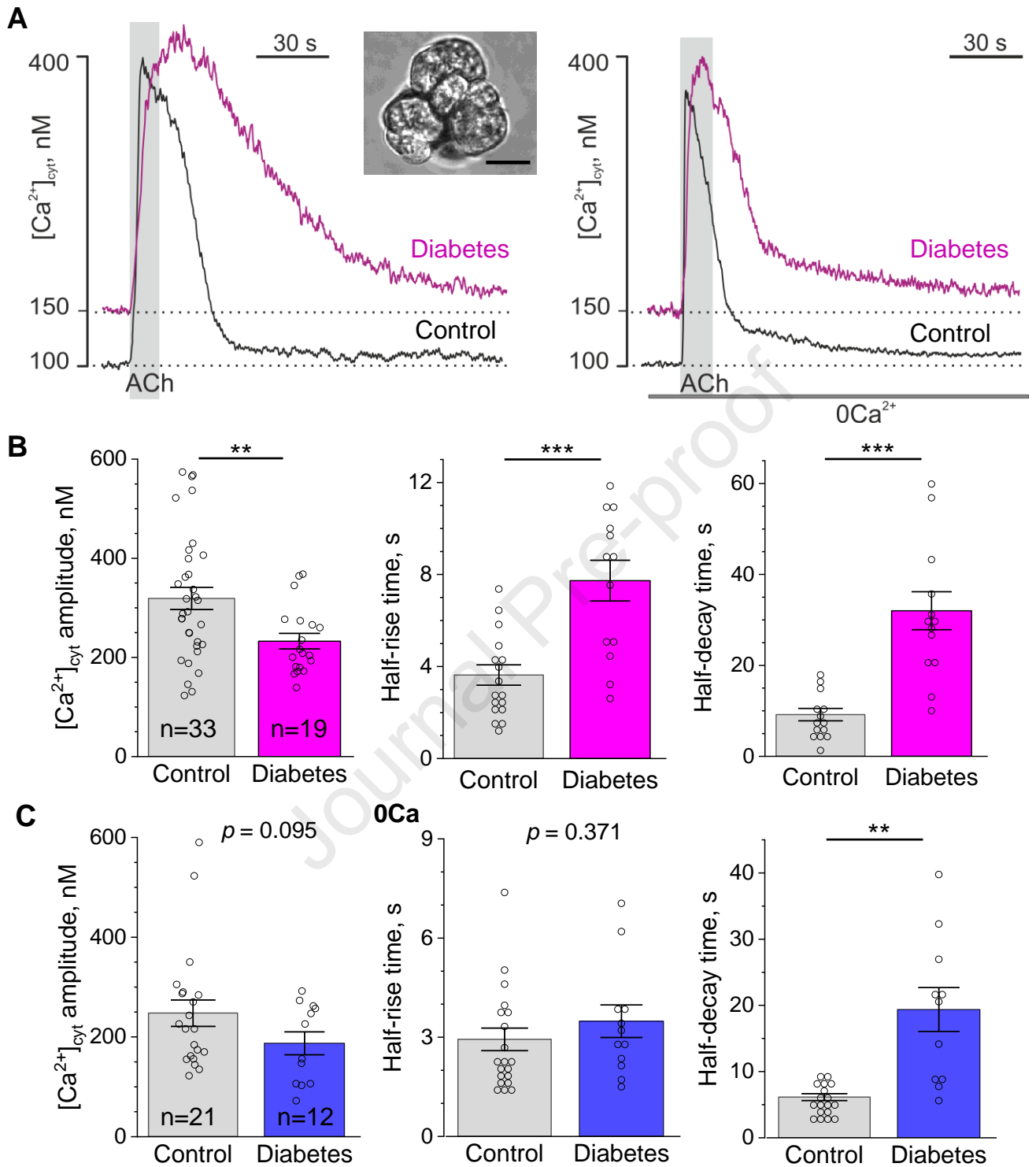


Figure 2

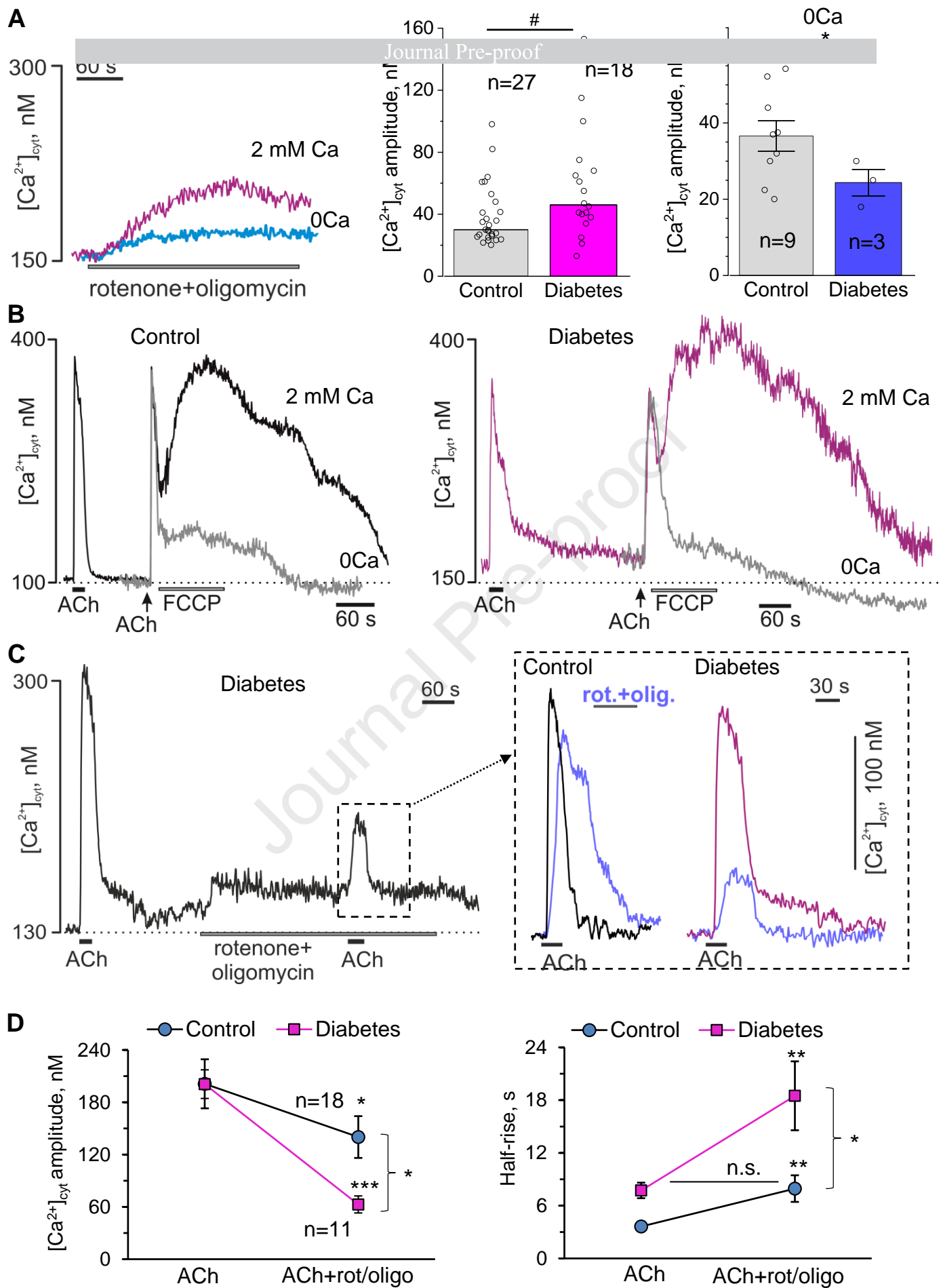


Figure 3

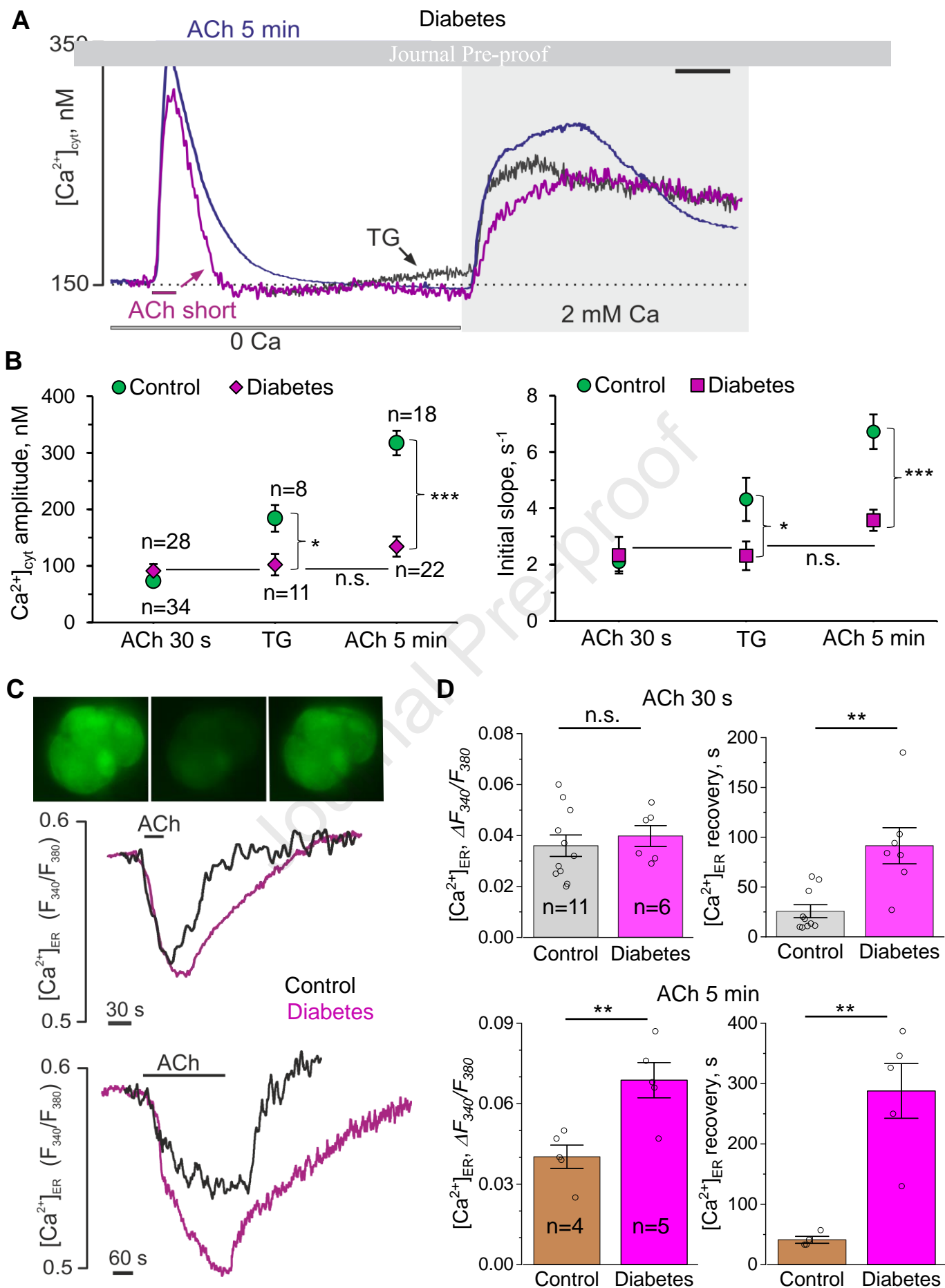


Figure 4

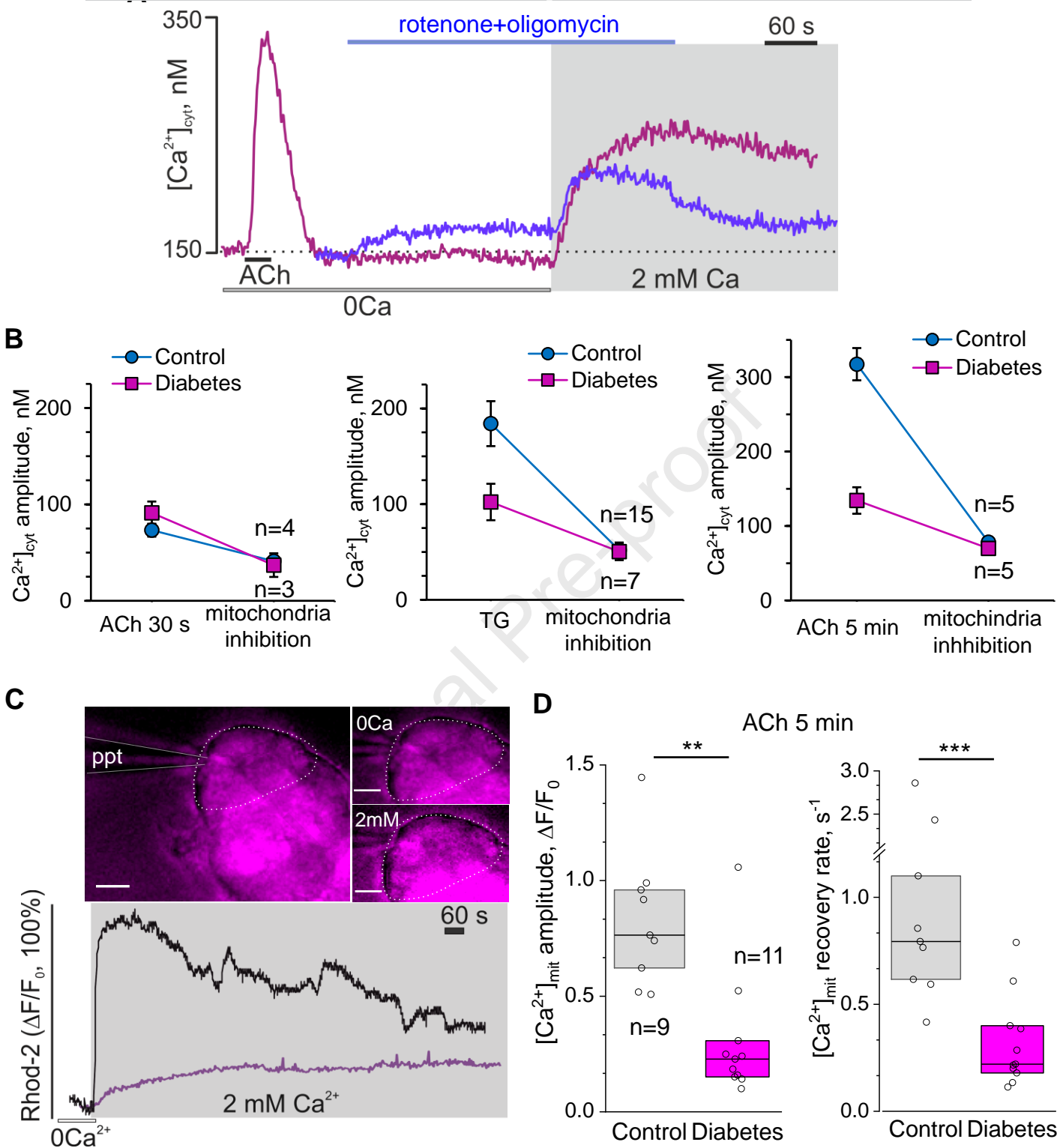


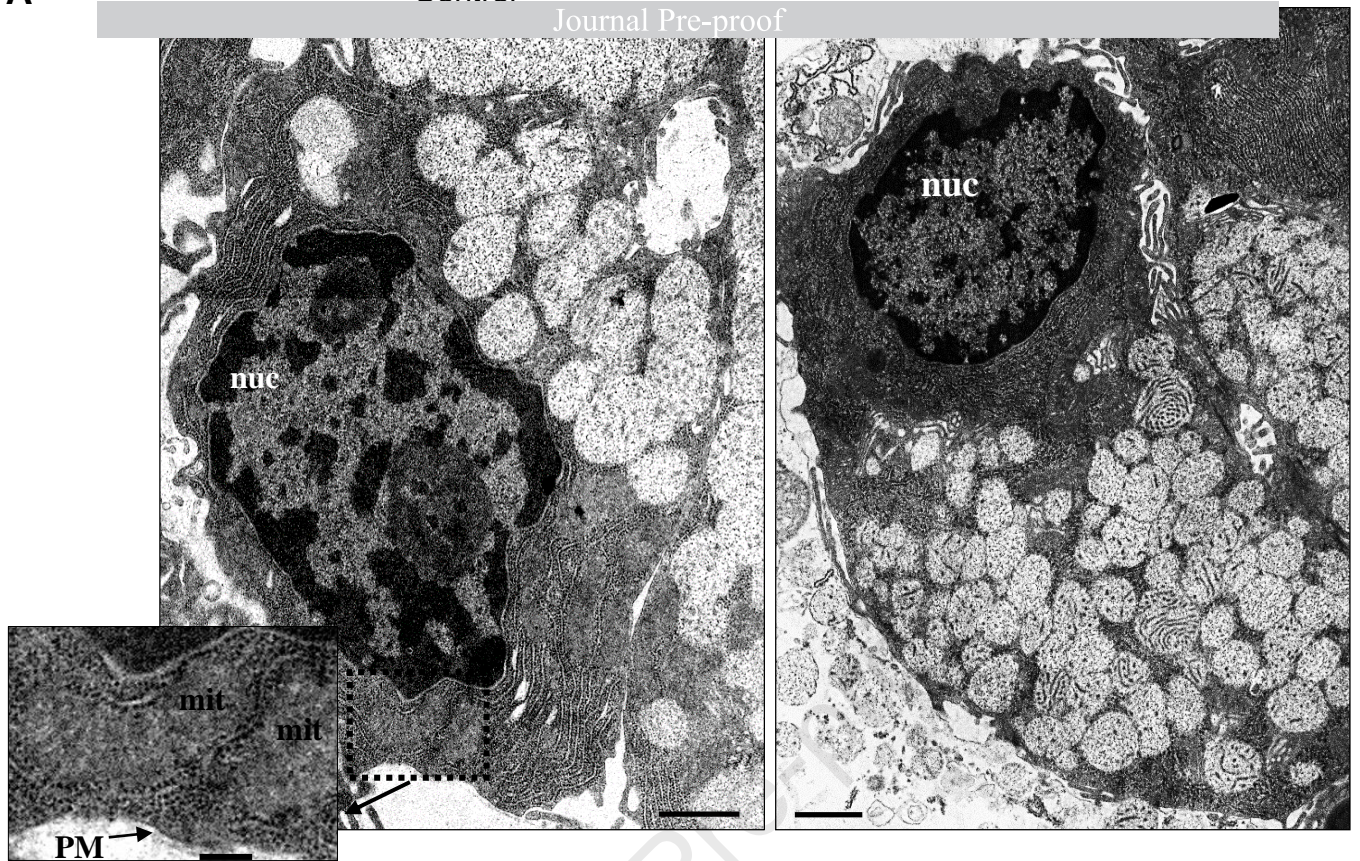
Figure 5

A

Control

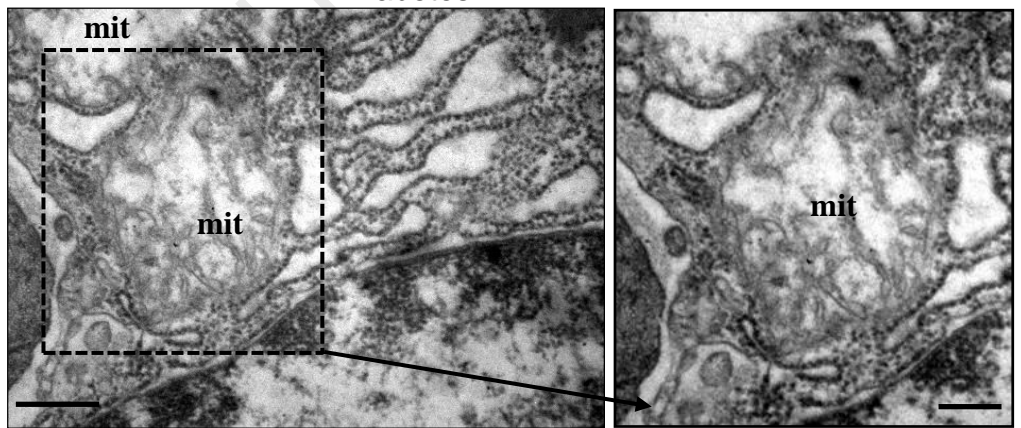
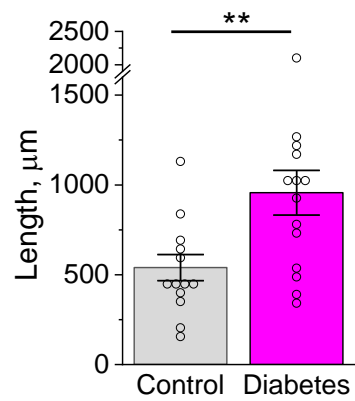
Diabetes

Journal Pre-proof

**B**

Basal membrane

Diabetes



Mitochondria

Diabetes

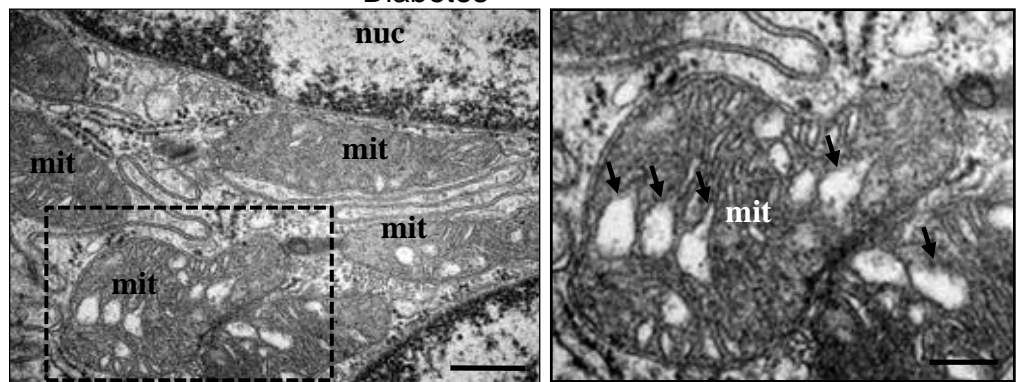
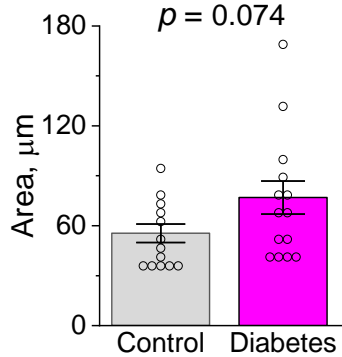
 $p = 0.074$ 

Figure 6

Highlights

- Submandibular gland dysfunction primarily contributes to xerostomia in diabetes.
- Saliva fluid hyposalivation remains resistant to cholinergic stimulation.
- Diabetes impairs cholinergic-induced Ca^{2+} signals in submandibular acinar cells.
- Malfunctioning mitochondria fail to maintain store-operated Ca^{2+} entry.
- Mitochondria display structural damage in diabetic xerostomia.

Journal Pre-proof

Declaration of interest: none.

Journal Pre-proof